SPECIAL FEATURE

Transparent antifouling material for improved operative field visibility in endoscopy

Steffi Sunny[a,1], George Cheng[b,1], Daniel Daniel[a], Peter Lo[b], Sebastian Ochoa[b], Caitlin Howell[a,c,d], Nicolas Vogel[e], Adnan Majid[b], and Joanna Aizenberg[a,d,f,g,2]

[a]John A. Paulson School of Engineering and Applied Sciences, Harvard University, Cambridge, MA 02138; [b]Interventional Pulmonology, Beth Israel Deaconess Medical Centre, Boston, MA 02215; [c]Department of Chemical and Biological Engineering, University of Maine, Orono, ME 04469; [d]Wyss Institute for Biologically Inspired Engineering, Harvard University, Cambridge, MA 02138; [e]Institute of Particle Technology and Interdisciplinary Center for Functional Particle Systems, Friedrich-Alexander University Erlangen-Nürnberg, 91058 Erlangen, Germany; [f]Department of Chemistry and Chemical Biology, Harvard University, Cambridge, MA 02138; and [g]Kavli Institute for Bionano Science and Technology, Harvard University, Cambridge, MA 02138

Edited by John A. Rogers, University of Illinois, Urbana, IL, and approved August 19, 2016 (received for review April 26, 2016)

Camera-guided instruments, such as endoscopes, have become an essential component of contemporary medicine. The 15–20 million endoscopies performed every year in the United States alone demonstrate the tremendous impact of this technology. However, doctors heavily rely on the visual feedback provided by the endoscope camera, which is routinely compromised when body fluids and fogging occlude the lens, requiring lengthy cleaning procedures that include irrigation, tissue rubbing, suction, and even temporary removal of the endoscope for external cleaning. Bronchoscopies are especially affected because they are performed on delicate tissue, in high-humidity environments with exposure to extremely adhesive biological fluids such as mucus and blood. Here, we present a repellent, liquid-infused coating on an endoscope lens capable of preventing vision loss after repeated submersions in blood and mucus. The material properties of the coating, including conformability, mechanical adhesion, transparency, oil type, and biocompatibility, were optimized in comprehensive in vitro and ex vivo studies. Extensive bronchoscopy procedures performed in vivo on porcine lungs showed significantly reduced fouling, resulting in either unnecessary or ∼10–15 times shorter and less intensive lens clearing procedures compared with an untreated endoscope. We believe that the material developed in this study opens up opportunities in the design of next-generation endoscopes that will improve visual field, display unprecedented antibacterial and antifouling properties, reduce the duration of the procedure, and enable visualization of currently unreachable parts of the body, thus offering enormous potential for disease diagnosis and treatment.

antifouling materials | endoscopy | surface wetting | biopsy

Camera-guided instruments are extensively used in a variety of applications such as oil field and marine exploration, sanitation inspections, robotics, optical sensors, and medicine. However, their operation is heavily compromised in highly contaminating environments where oil, sewage, marine fouling, or body fluids permanently disrupt the visual field. Clearance methods developed for these applications are insufficient in keeping the operative field functional and periodically cleaning the surfaces of these cameras for their continued effective performance is time consuming, costly, and often ineffective. The primary means used to clear lenses is mechanical wiping, in which case contours or curvature are particularly difficult to clean. Mechanical wiping can also damage and wear the lenses over time, and in scenarios involving a need to maintain attention to detail, damage can distort the view. Another approach to lens cleaning is to combine a camera with additional channels through which irrigation or spraying can be applied, significantly increasing the size of the instrument. Engineering a novel, antifouling, transparent material that can be applied to the surface of lenses may obviate contamination-induced vision loss, render cleaning procedures unnecessary, and allow miniaturization of the instrument for use in previously unreachable environments and confined spaces. Perhaps most significantly and more than in any industrial application, these challenges manifest themselves in medical procedures such as endoscopy.

Endoscope operators use the device to inspect interior regions of the human body and, in the case of flexible endoscopes, to obtain samples for diagnostic studies and to provide minimally invasive therapy via instruments passed through the working channel (1, 2). All these procedures bring the camera lens in close contact with body fluids, which adsorb onto the lens and compromise the visual field, risking imprecise or undesired movements of the device that damage the surrounding tissue and harm the patient. Traditionally, the lens is cleared via suction, vigorous saline irrigation, or rubbing against the tissue walls (3–6). Often, the endoscope needs to be retracted and manually cleaned, which is more likely to occur during the most crucial points in a procedure, for example, during excessive blood flow caused by a biopsy. Rigid endoscopes do not have a working channel through which irrigation or suction can be performed, so rubbing or withdrawal to wipe clean are the only recourses. All these measures impose risks to the patient's health. Of particular concern are procedures in flexible bronchoscopy (7, 8), where wiping against the delicate tissue in the lungs can cause lens reocclusion, coughing reflexes, or even tissue damage. Suction in narrow airways can lead to luminal collapse, and saline irrigation brings liquids into airways and can dislodge previously formed clots leading to bleeding. Retracting the endoscope and wiping it clean results in periodic, highly undesired interruptions contributing to longer and potentially riskier procedures. Conversion to open surgery may even be required when complications arise from procedures performed while visually impaired (3).

Significance

Inspection devices are frequently occluded by highly contaminating fluids that disrupt the visual field and their effective operation. These issues are particularly striking in endoscopes, where the diagnosis and treatment of diseases are compromised by the obscuring of the operative field by body fluids. Here we demonstrate that the application of a liquid-infused surface coating strongly repels sticky biological secretions and enables an uninterrupted field of view. Extensive bronchoscopy procedures performed in vivo on a porcine model shows significantly reduced fouling, resulting in either unnecessary or ∼10–15 times shorter and less intensive lens clearing procedures compared with an untreated endoscope.

Author contributions: S.S., G.C., N.V., A.M., and J.A. designed research; S.S., D.D., and C.H. performed in vitro studies; G.C., P.L., S.O., and A.M. performed in vivo studies; S.S., N.V., and J.A. analyzed data; J.A. supervised the research; and S.S., G.C., D.D., N.V., and J.A. wrote the paper.

Conflict of interest statement: J.A. is the founder of a start-up SLIPS Technologies, Inc.

This article is a PNAS Direct Submission.

[1]S.S. and G.C. contributed equally to this work.

[2]To whom correspondence should be addressed. Email: jaiz@seas.harvard.edu.

This article contains supporting information online at www.pnas.org/lookup/suppl/doi:10.1073/pnas.1605272113/-/DCSupplemental.

To address these problems, it is important to design a material that exhibits a set of critical properties that are difficult to achieve in combination: not only should it satisfy the general requirements for coatings of medical devices (i.e., to be conformal, mechanically robust, biocompatible, and antimicrobial), it additionally has to display high transparency, extreme resistance to fouling by body fluids, and antifogging properties that will allow the maintenance of a clear visual field throughout the procedure. The last decade has witnessed significant development in the design of Lotus leaf-inspired superamphiphobic surfaces, which show repellency of various liquids (9, 10). However, the requirements to sustain repellency throughout an endoscopic procedure are extremely challenging because (*i*) direct contact with proteins, cells, and bacteria, as well as the formation of blood clots upon contact with an abiotic surface, compromise the performance of superhydrophobic surfaces (11, 12), and (*ii*) their transparency is not easily achievable. Recently, liquid-infused coatings, consisting of a porous structure infiltrated with a lubricant, have emerged as a new, alternative strategy for repellent materials (11, 13–17). The formation of a stable lubricant overlayer on the surface creates a dynamic slippery barrier that protects the underlying substrate from direct contact with polluted media, thus drastically lowering the adsorption of various serious contaminants including bacteria (18, 19) and proteins (20–22). This new, non-fouling material can be designed to perform under flow (23, 24), provide enhanced damage tolerance (15, 16) and self-healing capabilities (11), or be integrated with a vascularized network that secretes the lubricant to repair the interface (25, 26).

The characteristics of liquid-infused coatings may provide a potential solution to mitigate the performance concerns in endoscopes, especially because methodologies have been developed to create transparent coatings with efficient liquid repellency (16, 20–22, 27). Here, we design and explore the function of a liquid-infused coating applied on a bronchoscope lens during clinically relevant procedures. We extensively test the repellency and operative field view of the coated endoscopes in contact with blood, mucus, and airway secretions, optimize the physico-chemical properties of the lubricant and its interface with the underlying solid to maximize antifouling properties, and characterize the performance of the coating in vivo in a porcine animal model whose lungs are subjected to a set of widely applied bronchoscopy procedures. In our study, the coated endoscopes significantly outperformed the unmodified instruments, showing either no fouling or minor, transient lens occlusion, retaining sufficient field of view, and requiring at least ~10–15 times shorter lens cleaning procedures.

Results

We adopted a layer-by-layer deposition (28–30) protocol using 20-nm silica particles and poly(diallyldimethylammonium chloride) to create mechanically robust porous 100-nm-thick silica network on glass (21). The coating is strongly adhered to the substrate showing no delamination during adhesion tape tests (21). The feature sizes and porosity of the silica network render the material antireflective, and when infused with a liquid, it displays increased transparency compared with the underlying plain glass (21). This porous silica network infiltrated with varying oils was first characterized for performance in vitro and ex vivo using a 5.5-mm-diameter Eggsnow USB Borescope Endoscope Pipe Inspection Camera (*SI Appendix*, Fig. S1 A and B), similar in size to an Olympus Bronchoscope (EXERA BF-160) used in our subsequent clinical in vivo experiments (*SI Appendix*, Fig. S1*C*). We developed a protocol to create a disposable endoscope attachment by fixing a coated glass coverslip onto the endoscope lens via a polydimethylsiloxane (PDMS) adhesion layer (Fig. 1*A* and *SI Appendix*, Fig. S1). For in vivo studies, a 6-mm glass coverslip was cut in the shape of a crescent to fit over the lens while leaving the working channel exposed (Fig. 1 *A* and *B*). This strategy (*i*) maintains transparency, (*ii*) seals the endoscope lens from contaminating liquids, (*iii*) allows the use of the working channel for various procedures (e.g., suction, irrigation), and (*iv*) enables removal of the attachment after experiments, making multiple repeats possible.

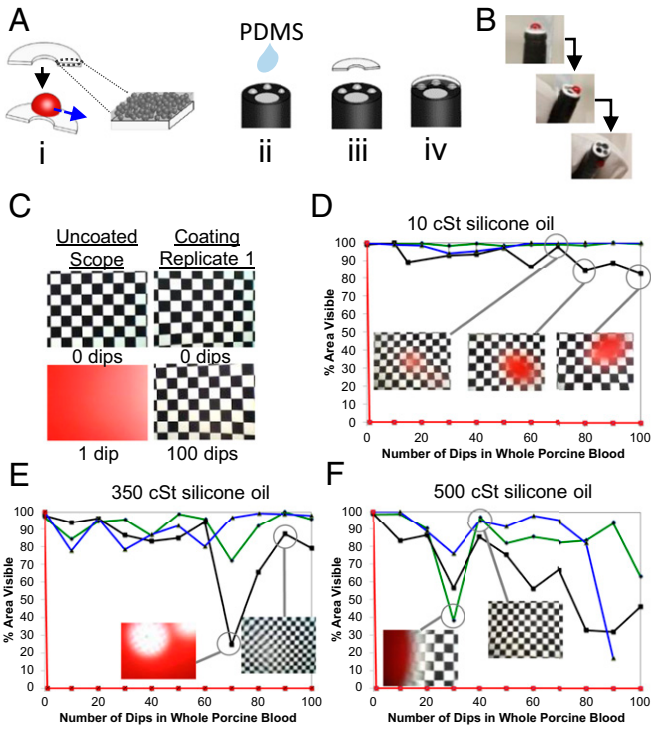

Fig. 1. Schematic of the coating process and subsequent characterization of the visual field during blood-dipping experiments with coated and untreated endoscopes. (*A*) An endoscope is modified with a disposable, glass coverslip (*i*) coated using previously described procedure (21). A drop of PDMS was added to the tip of the scope (*ii*) before fixing the coated glass on the endoscope lens (*iii*). The PDMS was cured securing the coverslip to the surface of the lens (*iv*) while exposing the working channel. (*B*) The coated endoscope repels a droplet of blood. (*C–F*) The following experiments were performed in triplicates. (Scale bar, insets in the plots are ~2 mm in width.) (*C*) The uncoated endoscope fails immediately after one dip in whole porcine blood (*Left*), whereas the 10-cSt oil allows for repellency up to 100 dips with no fouling (*Right*). (*D–F*) Evolution in the reduction in visible area as a function of the number of dips for endoscopes coated with silicone oils of varying viscosity: (*D*) 10 cSt; (*E*) 350 cSt; and (*F*) 500 cSt. The red lines correspond to the uncoated endoscopes. Replicates = 1 (green), 2 (blue), and 3 (black) correspond to each coated scope tested. *Insets* in *D* demonstrate visualization of field of view at 70, 80, and 100 dips for the poorest performing sample. The droplets of blood on the 350- and 500-cSt silicone oil surfaces are not as mobile due to viscous dissipation in the lubricant layer and temporary visual aberrations become more pronounced once they are shed from the surface. This contributes to the oscillatory behavior in visibility.

The reduction in performance for liquid-infused coatings is expected when the contaminating liquid comes into contact with and is irreversibly pinned on the underlying solid substrate. This contact can either happen catastrophically, when the liquid displaces the lubricant inside the silica network due to incompatible chemistry, or slowly with time, as the lubricant becomes depleted due to the formation of a wrapping layer around the repelled liquid and by shear force (23, 31). In the challenging environment in which endoscopes are used, highly adhesive body fluids will then contaminate the lens resulting in a reduction of the field of view and a necessity to clear the lens through extensive irrigation and suction. To estimate the duration of uncompromised lens performance in such conditions, we repeatedly immersed the endoscopes in and withdrew them from porcine blood and mucus and characterized the loss of visibility arising from the lens occlusion. We tested two classes of commercially available lubricants: silicone oils (Momentive or Gelest polydimethylsiloxanes) and perfluorinated fluids [perfluoroperhydrophenanthrene, or Vitreon, and perfluoropolyethers

(PFPEs): DuPont Krytox series]. These choices were dictated by the physical properties of these liquids (low surface energies and broad range of viscosities and volatilities), their chemical inertness, and prior US Food and Drug Administration (FDA)-approved applications of some of them in clinical settings, such as ophthalmic surgeries (32). The silicone oils of different viscosities (10, 350, and 500 cSt) showed stable performance and maintained a remarkably clear field of view after multiple dips of the endoscopes in fresh porcine blood (Fig. 1 *C*–*F*). In contrast, the untreated controls failed immediately after the first contact with blood (Fig. 1 *D*–*F*, red lines). The lowest viscosity silicone oil tested (10 cSt) consistently maintained a visual field close to 100% clarity for up to 100 dips in blood for all tested endoscopes (Fig. 1 *C* and *D*) (image analysis is described in *SI Appendix*, Fig. S2; Movie S1 presents an additional view of the resulting repellency properties).

Although there is natural variability among the different replicates (blue, black, and green lines in Fig. 1 *D*–*F* represent individual experiments performed with different samples), several observations can be made: the best sample (green line) demonstrates 100% clarity for all 100 dips (Fig. 1*D*), whereas the poorest performing sample (black line) only slightly fouls the lens (reduction in visibility by ∼20%). However, this fouling is found to be dynamic and transient in nature: droplets of size on the scale of millimeters are occasionally observed on the surface (Fig. 1*D*) but do not stay pinned; rather, they appear randomly in different areas and are easily removed by repeated dipping, bringing the field of view to the original 100% visibility. Importantly, we find that following contamination, after a gentle water wash and relubrication, the coating continues to maintain clarity for at least another 100 dips (*SI Appendix*, Fig. S3). We measured the force required to remove a 2-μL (millimeter-sized) blood droplet using a cantilever-based force sensor (*SI Appendix*, Fig. S4). For a silicone oil-based coating, it was found to be <10 μN, i.e., the weight of the droplet (∼20 μN) can easily overcome any pinning force leading to droplet self-removal (*SI Appendix*, Fig. S4). This low pinning force explains the mobility of the blood drop on the lens and the oscillatory nature of the experimentally measured field of view (Fig. 1*D*). Analogous oscillatory behavior in visualization is also found for the higher viscosity lubricants (Fig. 1 *E* and *F*), but temporary visual aberrations become more pronounced because the contaminating liquid is less mobile due to viscous dissipation in the lubricant layer (23, 33).

Perfluorinated lubricants, including FDA-approved Vitreon, were also investigated as alternatives to silicone oil. The pinning force for a droplet of blood measured on a force sensor for Vitreon-infused coating was >40 μN, exceeding the weight of the droplet by at least a factor of 2 (*SI Appendix*, Fig. S4). These results were further supported by optical observations and contact angle (CA) measurements of a blood droplet on these surfaces: the light passes through the interface between the blood droplet and the silicone oil-based coating indicating the presence of a stable lubricant film beneath the droplet and thus the absence of the direct contact between the contaminating medium and the substrate (CA = ∼180°); in contrast, for a Vitreon-based coating, the blood droplet is in direct contact with and pinned on the silica network, preventing any light from passing through (CA = ∼170°; *SI Appendix*, Fig. S4). Therefore, although perfluorinated liquid-based coatings show improved repellency compared with that of the unmodified scopes, they display reduced droplet mobility and tend to fail faster than their silicone oil-based analogs (after ∼5, 20, and 30 dips for Vitreon, 80-cSt PFPE, and 550-cSt PFPE, respectively; *SI Appendix*, Fig. S4–S7). Thus, moving forward we chose to focus on the silicone oil coating due to its superior performance in these tests.

Similar to the blood dip experiments, we immersed the silicone oil-coated endoscopes into porcine mucin solutions with a concentration (17 wt./vol%) typically found in cystic fibrosis patients: a patient population known to have an excess of extremely sticky lung secretions (34, 35). Fig. 2 clearly shows that the mucus is more easily shed from the surface lubricated with 10-cSt oil compared with the one lubricated with 350-cSt oil, surviving on average ∼20 dips before loss of visual field. Both coating types significantly outperform the uncoated control, which consistently loses visibility after the very first exposure to mucus solution (Fig. 2 *A* and *B*, red lines). Interestingly, in some cases, even with such a sticky contaminant, both the 10- and 350-cSt oil display an oscillatory behavior in vision reduction. We note that mucus is a viscoelastic liquid that cannot be easily shed from the lens surface from gravity alone, which results in some noise in the data between different coated samples. Importantly, however, up to ∼10 dips neither replicates of 10-cSt lubricated scopes lose more than ∼25% of the visual field, providing sufficient level of visualization. The field of view can also be restored after initial fouling by applying continued solution contact (*Insets* in Fig. 2*A*).

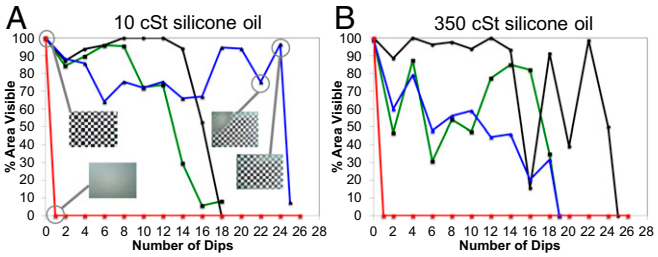

Fig. 2. Characterization of the visual field during mucus exposure. All experiments were performed in triplicates. Replicates = 1 (blue), 2 (green), and 3 (black) and correspond to each sample tested; red dots illustrate the performance of an uncoated control that fails after the first exposure. Dipping was performed in 17 wt.% mucin solution using endoscopes coated with 10-cSt silicone oil (*A*) and 350-cSt silicone oil (*B*). Note an oscillatory behavior in clearance, mostly pronounced for the higher viscosity oil.

To minimize the reduction in visual clarity due to lubricant trail formation and slower clearance that is observed for higher viscosity silicone oils while maximizing their possible contribution to longevity, we studied the performance of the coatings lubricated with the mixture of high and low viscosity oils. As an example, *SI Appendix*, Fig. S8 shows the results for the coating infused with a 10- and 350-cSt silicone oil in a 1:1 volume ratio. The mixed lubricant has a viscosity of 72 cSt and leads to approximately four times longer performance compared with the 10-cSt control (*SI Appendix*, Fig. S8*A*), showing that the performance can be further optimized by the application of a mixed-oil system.

To assess potential toxicity of the components of the coating, we subjected mouse mesenchymal stem cells in two separate sets of experiments to the two key components of the coating, i.e., 20-nm silica particles and lubricants (silicone or fluorinated oils). Fig. 3*A* shows live/dead stains of cells incubated with varying concentrations of silica nanoparticles. We quantify toxicity by evaluating the area coverage of cells (Fig. 3*C* and *SI Appendix*, Fig. S9). At the lowest concentration studied, 0.003 wt.%, that is more than four times higher than in the hypothetical worst case scenario in which the entire coating delaminates from the substrate (corresponding to $\sim 7 \times 10^{-4}$ wt.% of silica particles), we observe minimal dead cells and a live-cell coverage similar to the control, indicating no toxic effects from the silica particles (this concentration falls in the regime indicated by the dotted box in Fig. 3*C*). Toxicity begins to manifest itself only at a silica particle concentration ∼35 times higher than that available from the fully delaminated coating. It is noteworthy that the assembled coating provides a very strong bonding of the particles to the substrate (21), making any removal of nanoparticles from the coating due to mild abrasions with soft tissue extremely unlikely. Cells were then grown on a plain glass substrate and on the silicone oil-infused coating for 4 d to assess toxicity of the lubricant (Fig. 3 *B* and *D*). Although cells on the liquid-infused coating show lower

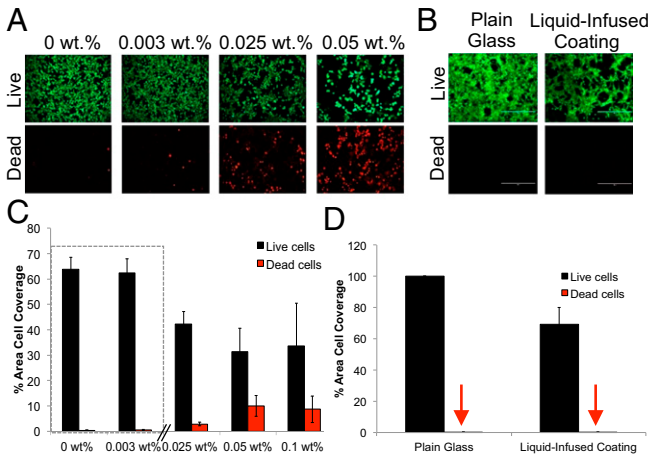

Fig. 3. Assessing the potential toxicity of the two components of the coating: silica nanoparticles and silicone oil. (*A*) Mouse mesenchymal stem cells were grown in tissue culture wells in the presence of varying concentrations of 20-nm silica particles and stained for live/dead cells. (*B*) The cells were grown on plain glass and on the silicone oil-infused coating and stained for live/dead cells. There are no visible dead cells on the control and the coating. (*C*) Quantification of area coverage with live (black) and dead (red) cells. In the concentration regime of interest (indicated by dashed box), no toxicity is detected, and coverage remains equal to the control. The coverage of dead cells increases to a measurable quantity only at concentrations that are 35 times higher than the regime of interest. (*D*) Similar quantification is also performed for cells grown on plain glass surfaces versus liquid-infused surfaces. The number of dead cells is negligible on the coating, as well as on the plain glass control.

cell coverage (as expected from the compromised adhesion to the repellent coating), the number of dead cells are negligible (Fig. 3*D*). The effect of the PFPE oil was also evaluated and found to be nontoxic (*SI Appendix*, Fig. S10).

Subsequent microbial adhesion tests in which *Escherichia coli* was grown for 24 h on a coated glass slide show significantly reduced bacterial film overgrowth compared with an uncoated control (*SI Appendix*, Fig. S11). The 24-h incubation time is much longer than any anticipated endoscopic procedure; therefore, we are confident that our coating can prevent bacterial attachment in procedures performed in a shorter length of time. We also evaluated vision loss after contact with cellular debris (*SI Appendix*, Fig. S12), in low pH conditions (*SI Appendix*, Fig. S13), and after scratching (*SI Appendix*, Fig. S14), which are scenarios often encountered in various endoscopic procedures, and found no substantial reduction in performance.

To determine the efficacy of the surface coating in maintaining a clear operative field, we performed bronchoscopy in ex vivo and in vivo porcine lung models. The porcine model is frequently used in pulmonary research due to its similarities to humans in size and bronchial structures (36). First, we used an explanted porcine lung to test the function and resistance of a coated endoscope against lung surfactant, present to preserve lung compliancy (37). Due to its interfacial activity lung surfactant may compromise the coating's stability and contribute to impaired vision and fouling. After contact with airway secretions in the explanted lung, the uncoated endoscope was unable to retain a clear field of vision, whereas the coated scope maintained complete clarity (Fig. 4*A* and Movie S2). This encouraging result strongly indicates that the antifouling liquid-infused coating may indeed offer significant advantages in clinically important in vivo procedures, which we investigated next.

For this part of our study, we evaluated the performance during typical bronchoscopy procedures, such as airway inspections, endobronchial biopsies, and transbronchial biopsies, performed by pulmonologists in vivo on porcine lungs. The results are presented in Movies S3–S5 and extracted as images in Fig. 4. In all of the procedures, the likelihood of vision loss of a coated endoscope after contact with biological material is reduced by at least a factor of 2 compared with the uncoated reference (the control lost vision in ∼50% of all contacts, the coated endoscope in less than 20% and the vision loss in the latter case was partial and often transient). Moreover, these experiments are likely to have overestimated the quality of the uncoated control because residual silicone oil present in the intubation tube at entry points from the previous experiments with coated endoscopes may have deposited on the control in subsequent experiments, improving its operation.

The most striking difference in performance between the liquid-infused coating and the uncoated bronchoscope is observed during endobronchial biopsies where forceps are used to sample the carina. After withdrawal of the forceps, contact of the bronchoscope with the bleeding carina induces complete vision loss. Fig. 4*B* summarizes the results comparing the coated and uncoated instruments when both bronchoscopes were exposed to similar levels of bleeding. Of the three times that the biopsy was performed, the uncoated bronchoscope lost visibility all three times (Fig. 4*B* and Movie S3). Clearance on average took more than 1 min. In two instances, visibility was not completely retained even after intermittent rubbing and suction, leading to blind operation for more than 2 min. In contrast, the bronchoscope coated with the liquid-infused material maintained a clear field of vision (biopsy 1) or, if partial vision loss had occurred, visibility was restored rapidly (on average, in just 4 s) and with minor efforts (short contact with the wall or short suction to remove pooled blood) (Fig. 4*B* and Movie S4).

After a transbronchial biopsy (Movie S5) with the coated bronchoscope, significant bleeding necessitated the performance of a wedge; a procedure in which the bronchoscope is pressed against the bleeding site to form a plug that stops the blood flow and facilitates clotting to induce hemostasis. After two submersions in blood for ∼5 s, the field of vision remained completely clear (Fig. 4 *C*, *i*). Extensive suction (∼20 s) applied to remove the blood from the surrounding area before the wedge resulted in ∼50% fouling of the lens area and partial loss in vision (Fig. 4 *C*, *ii*). However, clarity was sufficient to allow the operator to visualize the airway, guide the bronchoscope to the site of bleeding, and perform the wedge in this critical situation involving bronchoscope exposure to a substantial amount of blood and to shear conditions imposed by the suction procedure. After 3 min, the bronchoscope was withdrawn from the bleeding site, and remarkably, more than 50% of the visual field remained clear, with occlusion occurring exclusively at the edge of the lens (quite likely due to edge effects whereby blood adherence starts on the uncoated sides of the endoscope). Short contact with the airway wall and suction completely clears the lens within seconds (Fig. 4 *C*, *ii*). This exceptional performance of the coated endoscope during extensive bleeding demonstrates the potential of the coating in one of the harshest environments encountered in bronchoscopy.

Beyond medical endoscopy, we demonstrate that the coating preserves full transparency on exposure to crude oil, sewage mimetic, and algae (*SI Appendix*, Fig. S15), showing its potential in camera-guided instruments used in sanitation, marine, and oil exploration.

Discussion

We demonstrated that liquid-infused repellent coatings can be used in camera-guided instruments to protect the lens from contamination and obstructed visibility. Such coatings applied on endoscope lenses provide unprecedented clarity of visual field after contact with a range of highly contaminating body fluids. In particular, a coating infused with 10-cSt silicone oil is shown to consistently repel blood when repeatedly submerged in it losing not more than 20% visibility, whereas the uncoated scope loses 100% of the field of view immediately after submersion. The former also drastically improves the repellency of mucus and lung surfactant. In vitro toxicity tests do not indicate any adverse effects. This coating was therefore tested in multiple bronchoscopies performed in vivo on porcine lungs. A range of clinically relevant procedures (endobronchial

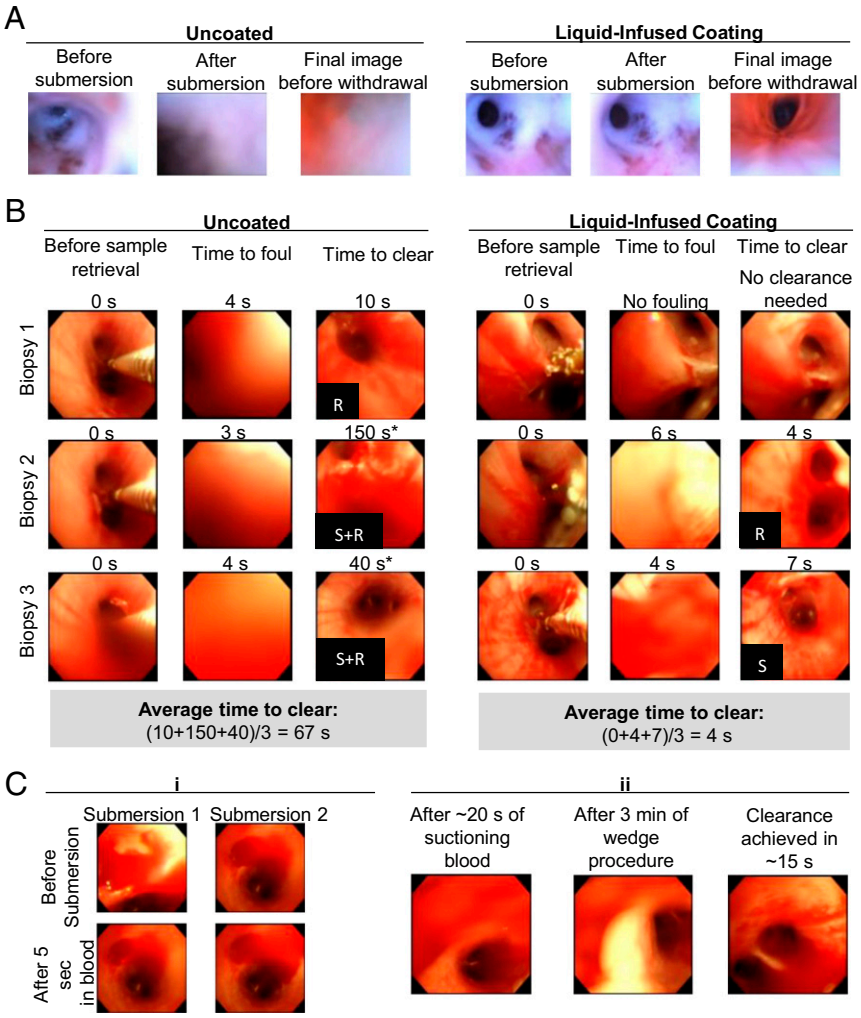

Fig. 4. Ex vivo and in vivo bronchoscopy procedures. (*A*) Contact of the endoscope with lung secretions in an ex vivo lung. (*B*) Endobronchial biopsies using an uncoated bronchoscope were performed in the right lung of a pig, whereas the liquid-infused coated bronchoscope sampled the left lung of the same animal. Methods used for the lens clearance are indicated on the bottom-left of the image: R, rubbing against airway walls; S, suction. The control endoscope fouls for all three biopsies with extensive suction and rubbing required for biopsies 2 and 3 (the symbol * in the "time to clear" indicates that even after intense clearance complete visibility was not regained). The average time for clearance for all three procedures was 67 s. The liquid-infused coating did not foul after the first biopsy and was quickly cleared using either suction or rubbing after the second and third biopsy with an average clearance time of 4 s. (*C*) Images obtained after performing a wedge. Visualization was entirely retained after two submersions in blood (*i*) and partially obstructed (~50% of clear field remained) after performing a 20-s blood suction and a 3-min wedge (*ii*).

biopsy, transbronchial biopsy, and transbronchial brushing) demonstrate that these antifouling liquid-infused coatings prevent loss of vision from blood occlusion and considerably reduce the clearance time needed to completely regain visibility, even in harsh environments involving strong bleeding. In contrast, the visual field of the uncoated endoscopes in both ex vivo and in vivo procedures are immediately compromised under the same experimental conditions and require extended (10–15 times longer) clearance times.

Solving lens fouling with a repellent, transparent surface coating has much broader implications in medicine, far beyond the improvement of visibility presented in this study. One particular consideration is that liquid-infused surfaces significantly reduce bacterial adhesion (18, 19, 24, 25, 38), which is a key advantage in endoscopy, considering the magnitude of the tragedy at the University of California, Los Angeles Medical Center, where seven patients were infected after the procedure with Carbapenem-resistant *Enterobacteriaceae* due to a lack of sufficient sterilization (39). More recently, outbreaks have occurred in hospitals in Seattle, Pittsburgh, and Chicago (40). We envision that in the future design of endoscopes, this coating can be applied directly to the endoscope lens or on a disposable cover. Direct application on the lens would require a simple relubrication after standard sterilization protocols, which would reduce bacterial adhesion and therefore possibility of infection.

Another potential consideration is the reduction in the duration of the procedure, with associated decrease in health care costs, and the increase in the number of treatments that could be performed. To put our results in perspective, for example, the time required for sample collection during a biopsy when no fouling occurs is only ~20–25 s. Therefore, the cleaning time after a fouling event in an uncoated bronchoscope (on average 67 s) is approximately two to five times the length of the sample collection duration, whereas in a coated endoscope, the cleaning time (on average 4 s) contributes only ~1/5th to the sample collection time. The total duration of one endobronchial biopsy from entry into the intubation channel to exit is ~1 min. These values indicate that physicians spend approximately equal time cleaning the lens as the total procedure in an uncoated bronchoscope, whereas in a coated instrument the cleaning adds merely 5–10% to the total procedure time and in many cases is not needed at all.

We have chosen bronchoscopy as one of the most challenging cases of medical endoscopy, in which highly delicate lung tissue with complex air/liquid interfaces is involved and thus common approaches of lens wiping, irrigation, and suction can lead to serious complications, including tissue injury, lung collapse, or dislodging of clots in the irrigated airways. Therefore, minimizing the use of the cleaning procedures, as shown in this study, will result in potential improvement in safety by decreasing the probability of tissue damage and associated complications, as well as of patient discomfort. The lubricated surface of the instrument is likely to further reduce discomfort during insertion and removal of the endoscope. There are also additional corner cases where this coating may be used, such as low pH environments encountered in gastroenterology.

Finally, it is important to emphasize the growing interest in miniaturized endoscopes that may enable the visualization of the most inaccessible regions of the human body. Further miniaturization of currently used scopes is impossible, as it will necessitate the elimination of the working channel, leaving doctors without the recourse of suction and irrigation to clear the visual field. Our results show that immersion in blood, mucus and secretions enable an uninterrupted airway inspection with the coated scope. The presence of such a coating may thus offer an unprecedented opportunity to design a flexible instrument without working channels, reducing its size to 2–3 mm, approximately the diameter of unimaged small airways. We believe therefore that liquid-infused coatings may provide a strategy to significantly expand the limits of the areas of the human body that physicians can currently image, offering enormous potential for improving disease diagnosis and treatment.

Although we chose to focus on a medical application, the findings of this study extend to the use of these coatings in other industries. The exceptional antifouling performance of this class of transparent materials has the potential to mitigate the effects of vision loss from highly contaminating liquids on inspection cameras in sewers for sanitation systems, oil field and underwater exploration, robotics, surveillance cameras, solar panels, and optical sensors. All these scenarios benefit from the improved visibility, reduction in cleaning times, and therefore decreased overall cost and enhanced functionality.

Materials and Methods

A 5.5-mm Eggsnow borescope was used to perform all blood and mucus dipping experiments. The toxicity studies were performed with OVA D1 mesenchymal stem cells. The in vivo bronchoscopy procedures were completed using an Olympus Bronchoscope (EXERA BF-160). The large animal study was approved by the Institutional Animal Care & Use Committee of Beth Israel Deaconess Medical Centre under Protocol 022-2015 (Performance of SLIPS-Bronchoscope in Swine Study). Detailed materials and methods are described in *SI Appendix, SI Materials and Methods*.

ACKNOWLEDGMENTS. We thank Dr. M. Aizenberg for helpful discussions; M. Duffy, F. Connolly, and B. Weinstein for assistance with image analysis; and C. Zhang for the algae solution. S.S. thanks the Natural Sciences and Engineering Research Council (NSERC) of Canada for financial support. N.V. acknowledges funding by the Deutsche Forschungsgemeinschaft through the Cluster of Excellence (EXC 315) and the Interdisciplinary Center for Functional Particle Systems (FPS) at Friedrich-Alexander University Erlangen-Nürnberg. This work was supported by the Wyss Institute for Biologically Inspired Engineering at Harvard University and National Science Foundation (NSF)Materials Research Science and Engineering Centers (MRSEC) Grant DMR-1420570.

1. Singh A, Donepudi I, Mundkur M, Levey J (2009) Endoscopy. *Am J Gastroenterol* 104 (S3):S500–S544.
2. Leffler DA, et al. (2010) The incidence and cost of unexpected hospital use after scheduled outpatient endoscopy. *Arch Intern Med* 170(19):1752–1757.
3. Lawrentschuk N, Fleshner NE, Bolton DM (2010) Laparoscopic lens fogging: A review of etiology and methods to maintain a clear visual field. *J Endourol* 24(6):905–913.
4. Bessel JR, Flemming E, Kunert W, Buess G (1996) Maintenance of a clear vision during laparascopic surgery. *Minim Invasive Ther Allied Technol* 5(5):450–455.
5. Flemming E, Bessel JR, Kunert W, Eibl H, Buess G (1996) Principles determining optical clarity in endoscopic surgery. *Minim Invasive Ther Allied Technol* 5(5):440–444.
6. Ohdaira T, Nagai H, Kayano S, Kazuhito H (2007) Antifogging effects of a socket-type device with the superhydrophilic, titanium dioxide-coated glass for the laparoscope. *Surg Endosc* 21(2):333–338.
7. Walters DM, Wood DE (2016) Operative endoscopy of the airway. *J Thorac Dis* 8(Suppl 2):S130–S139.
8. Márquez-Martín E, et al. (2010) Endobronchial administration of tranexamic Acid for controlling pulmonary bleeding: A pilot study. *J Bronchology Interv Pulmonol* 17(2):122–125.
9. Kota AK, Kwon G, Tuteja A (2014) The design and applications of superomniphobic surfaces. *NPG Asia Mater* 6(7):e109.
10. Li X-M, Reinhoudt D, Crego-Calama M (2007) What do we need for a superhydrophobic surface? A review on the recent progress in the preparation of superhydrophobic surfaces. *Chem Soc Rev* 36(8):1350–1368.
11. Wong T-S, et al. (2011) Bioinspired self-repairing slippery surfaces with pressure-stable omniphobicity. *Nature* 477(7365):443–447.
12. Friedlander RS, et al. (2013) Bacterial flagella explore microscale hummocks and hollows to increase adhesion. *Proc Natl Acad Sci USA* 110(14):5624–5629.
13. Lafuma A, Quéré D (2011) Slippery pre-suffused surfaces. *EPL* 96(5):56001.
14. Grinthal A, Aizenberg J (2014) Mobile interfaces: Liquids as a perfect structural material for multifunctional, antifouling surfaces. *Chem Mater* 26(1):698–708.
15. Tesler AB, et al. (2015) Extremely durable biofouling-resistant metallic surfaces based on electrodeposited nanoporous tungstite films on steel. *Nat Commun* 6:8649.
16. Vogel N, Belisle RA, Hatton B, Wong T-S, Aizenberg J (2013) Transparency and damage tolerance of patternable omniphobic lubricated surfaces based on inverse colloidal monolayers. *Nat Commun* 4:2167.
17. Kim P, Kreder MJ, Alvarenga J, Aizenberg J (2013) Hierarchical or not? Effect of the length scale and hierarchy of the surface roughness on omniphobicity of lubricant-infused substrates. *Nano Lett* 13(4):1793–1799.
18. Epstein AK, Wong T-S, Belisle RA, Boggs EM, Aizenberg J (2012) Liquid-infused structured surfaces with exceptional anti-biofouling performance. *Proc Natl Acad Sci USA* 109(33):13182–13187.
19. Li J, et al. (2013) Hydrophobic liquid-infused porous polymer surfaces for antibacterial applications. *ACS Appl Mater Interfaces* 5(14):6704–6711.
20. Leslie DC, et al. (2014) A bioinspired omniphobic surface coating on medical devices prevents thrombosis and biofouling. *Nat Biotechnol* 32(11):1134–1140.
21. Sunny S, Vogel N, Howell C, Vu TL, Aizenberg J (2014) Lubricant-infused nanoparticulate coatings assembled by layer-by-layer deposition. *Adv Funct Mater* 24(42):6658–6667.
22. Manabe K, Kyung K-H, Shiratori S (2015) Biocompatible slippery fluid-infused films composed of chitosan and alginate via layer-by-layer self-assembly and their antithrombogenicity. *ACS Appl Mater Interfaces* 7(8):4763–4771.
23. Howell C, et al. (2015) Stability of surface-immobilized lubricant interfaces under flow. *Chem Mater* 27(5):1792–1800.
24. MacCallum N, et al. (2015) Liquid-infused silicone as a biofouling-free medical material. *ACS Biomater Sci Eng* 1(1):43–51.
25. Howell C, et al. (2014) Self-replenishing vascularized fouling-release surfaces. *ACS Appl Mater Interfaces* 6(15):13299–13307.
26. Cui J, Daniel D, Grinthal A, Lin K, Aizenberg J (2015) Dynamic polymer systems with self-regulated secretion for the control of surface properties and material healing. *Nat Mater* 14(8):790–795.
27. Nishioka S, et al. (2016) Facile design of plant-oil-infused fine surface asperity for transparent blood-repelling endoscope lens. *RSC Adv* 6(53):47579–47587.
28. Decher G, Hong JD, Schmitt J (1992) Buildup of ultrathin multilayer films by a self-assembly process: III. Consecutively alternating adsorption of anionic and cationic polyelectrolytes on charged surfaces. *Thin Solid Films* 210-211:831–835.
29. Krogman KC, Lowery JL, Zacharia NS, Rutledge GC, Hammond PT (2009) Spraying asymmetry into functional membranes layer-by-layer. *Nat Mater* 8(6):512–518.
30. Hiller J, Mendelsohn JD, Rubner MF (2002) Reversibly erasable nanoporous antireflection coatings from polyelectrolyte multilayers. *Nat Mater* 1(1):59–63.
31. Smith JD, et al. (2013) Droplet mobility on lubricant-impregnated surfaces. *Soft Matter* 9(6):1772–1780.
32. Barca F, Caporossi T, Rizzo S (2014) Silicone oil: Different physical proprieties and clinical applications. *BioMed Res Int* 2014:502143.
33. Daniel D, Mankin MN, Belisle RA, Wong T-S, Aizenberg J (2013) Lubricant-infused micro/nano-structured surfaces with tunable dynamic omniphobicity at high temperatures. *Appl Phys Lett* 102(23):231603.
34. Donaldson SH, et al. (2006) Mucus clearance and lung function in cystic fibrosis with hypertonic saline. *N Engl J Med* 354(3):241–250.
35. Henderson AG, et al. (2014) Cystic fibrosis airway secretions exhibit mucin hyperconcentration and increased osmotic pressure. *J Clin Invest* 124(7):3047–3060.
36. Rogers CS, et al. (2008) The porcine lung as a potential model for cystic fibrosis. *Am J Physiol Lung Cell Mol Physiol* 295(2):L240–L263.
37. Griese M (1999) Pulmonary surfactant in health and human lung diseases: State of the art. *Eur Respir J* 13(6):1455–1476.
38. Yuan S, Luan S, Yan S, Shi H, Yin J (2015) Facile fabrication of lubricant-infused wrinkling surface for preventing thrombus formation and infection. *ACS Appl Mater Interfaces* 7(34):19466–19473.
39. Health U (2015) UCLA statement on notification of patients regarding endoscopic procedures. Available at https://www.uclahealth.org/news/ucla-statement-on-notification-of-patients-regarding-endoscopic-procedures. Accessed December 10, 2015.
40. Eisler P (2015) Deadly bacteria on medical scopes trigger infections. *USA Today*. Available at www.usatoday.com/story/news/2015/01/21/bacteria-deadly-endoscope-contamination/22119329/. Accessed December 30, 2015.

Supporting Information

Sunny et al. 10.1073/pnas.1605272113

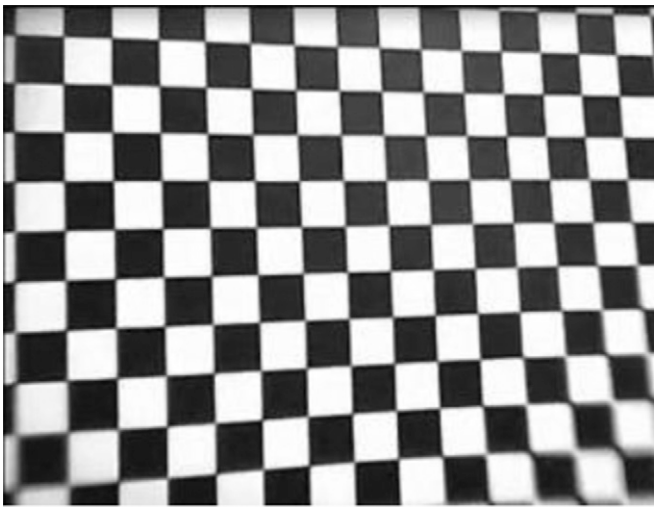

Movie S1. Blood dipping.

Movie S1

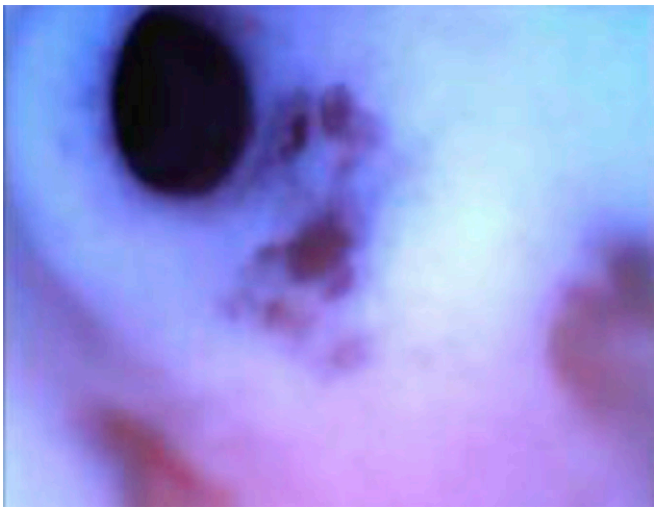

Movie S2. Airway inspection.

Movie S2

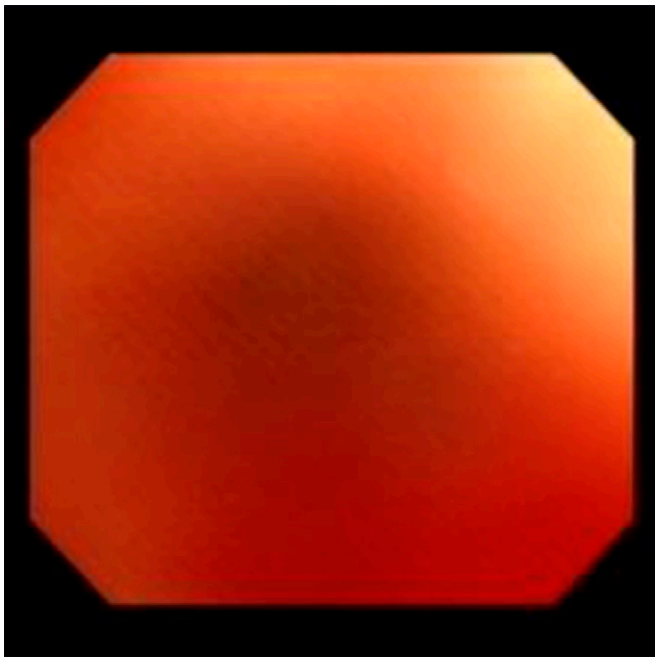

Movie S3. Endobronchial biopsy/control, uncoated scope.

Movie S3

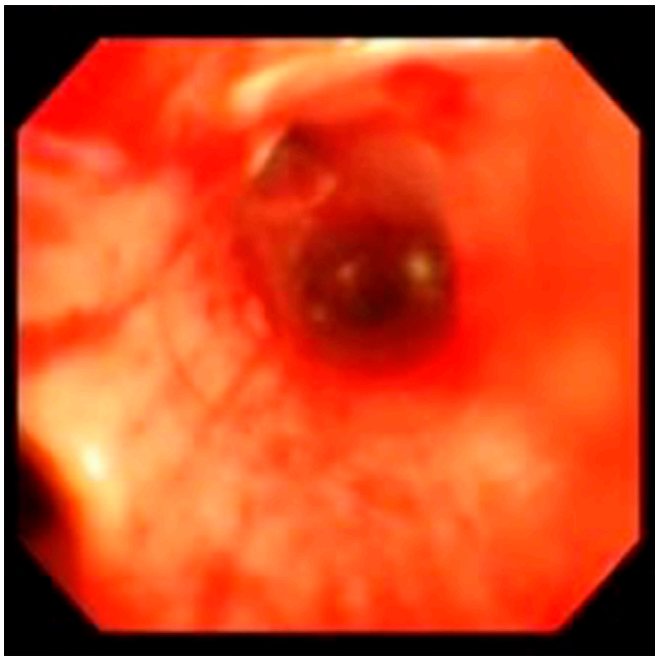

Movie S4. Endobronchial biopsy/liquid-infused coating.

Movie S4

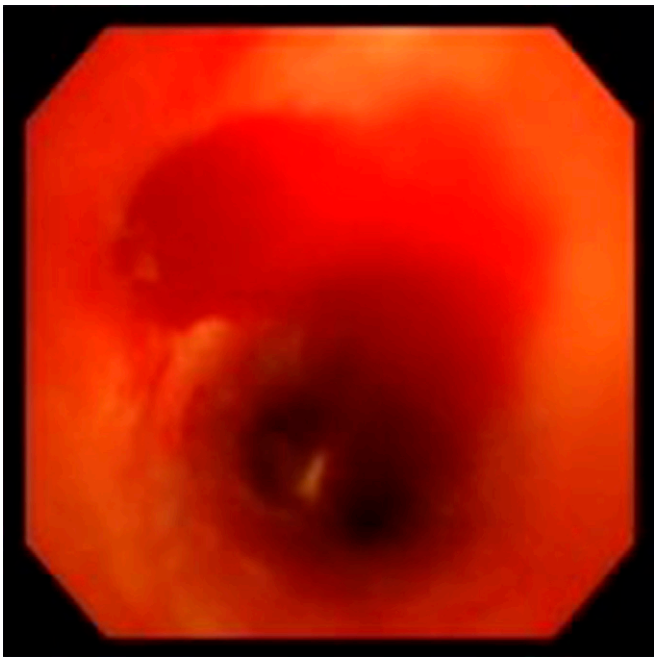

Movie S5. Bleeding after transbronchial biopsy.

Movie S5

Other Supporting Information Files

SI Appendix (PDF)

Supporting Information

Transparent Antifouling Material for Improved Operative Field Visibility in Endoscopy

Steffi Sunny,[1*] George Cheng,[2*] Daniel Daniel[1], Peter Lo,[2] Sebastian Ochoa,[2] Caitlin Howell,[1,3,4] Nicolas Vogel,[5] Adnan Majid[2] and Joanna Aizenberg[1,4,6,7]

*co-first authored

[1]John A. Paulson School of Engineering and Applied Sciences, Harvard University, Cambridge, MA,02138; [2]Interventional Pulmonology, Beth Israel Deaconess Medical Centre, Boston, MA 02215; [3]Department of Chemical and Biological Engineering, University of Maine, Orono, ME 04469; [4]Wyss Institute for Biologically Inspired Engineering, Harvard University, Cambridge, MA 02138; [5]Institute of Particle Technology and Interdisciplinary Center for Functional Particle Systems (FPS) Friedrich-Alexander University Erlangen-Nürnberg, Haberstr. 9a, 91058 Erlangen, Germany; [6]Department of Chemistry and Chemical Biology, Harvard University, Cambridge, MA 02138; [7]Kavli Institute for Bionano Science and Technology, Harvard University, Cambridge, MA 02138

Contents:

Available Videos:

1. Materials and Methods

Preparation of the coated coverslips

6 mm circular glass coverslips were cut from a square 1" x 2" square coverslip (0.16-0.19 mm thickness) using a diamond scriber. Glass substrates were treated with oxygen plasma (Model femto, Plasma Diener, Germany) for 2 min with 10 sccm oxygen gas flow and 100W power to activate the silica surface. The layer-by-layer deposition was performed by immersion of the substrates in a 0.1 wt.-% solution of poly(diallyldimethylammonium) chloride (PDADMAC) for 10 min, followed by rinsing in DI water three times for 30 s and subsequent immersion into a solution of 0.1 wt.-% Ludox silica colloids for 10 min and rinsing for 30 s in water three times. This cycle was repeated to deposit 20 multilayers using the nanoStrata Inc. dip coater. The organic material was removed by combustion at 500 °C (ramped from room temperature to 500 °C for 5 h, 2 h at 500°C, ramped from 500°C back to room temperature in 5 h. The resulting porous glass/silica coatings were functionalized by vapor-phase deposition of (1H,1H,2H,2H-tridecafluorooctyl)-trichlorosilane (abbreviated as 13F below – functionalization for infusion with perfluorocarbon oils) or n-decyltrichlorosilane (functionalization for infusion with silicone oil) for 24 h at reduced pressure and room temperature. Prior to silanization, the substrates were plasma-treated with oxygen plasma for 2 min with 10 sccm oxygen gas flow and 100W power.

Attachment of the coverslip to the endoscope

Poly(dimethylsiloxane) (PDMS) was prepared at a 10:1 ratio of elastomer to curing agent using the Sylgard 184 Silicone Elastomer Kit. Bubbles were eliminated after mixing using a vacuum chamber. A drop of PDMS was applied to the tip of the scope and the coverslip gently placed on top. The PDMS was allowed to cure at room temperature for 48 h prior to use.

Lubrication

3 µl of DuPont's perfluoropolyether (PFPE) oils (Krytox GPL 103 – kinematic viscosity 80 cSt at 20°C, 1.92 g/mL at 0°C; Krytox GPL 105 – kinematic viscosity 550 cSt at 20°C, 1.94 g/mL at 0°C), Fluoromed's perfluoroperhydrophenanthrene (APF-215M Vitreon – kinematic viscosity 8 cSt at 25°C, 2.02 g/mL at 25°C), Momentive's silicone oil (20 cSt at 25°C) or Gelest's silicone oil (DMST23 - 350 cSt at 25°C) was added to the coverslip until uniform coverage was achieved by tilting. Holding a kim wipe to the edge of the coverslip and allowing the lubricant to absorb in to the kim wipe removed excess lubricant.

Blood dipping experiments

Fresh porcine blood (Na Heparinized from Lampire Biological Laboratories) was incubated for 30 min in a 37°C cell culture incubator prior to the experiment. A coated Eggsnow Borescope endoscope (5.5 mm diameter, 2 m length) was dipped in the blood (~1 s per dip) and withdrawn. The image clarity was determined by visualizing a checkerboard pattern every ten dips. The image analysis is described in detail in Chapter 3 below.

Mucin dipping experiments

Mucin powder from porcine stomach lining type II (Sigma Aldrich) was resuspended in 1x Phosphate Buffered Saline at 17 wt./vol %. The solution was vortexed gently for 1 h to ensure

complete mixing. Coated Eggsnow scopes (5.5 mm diameter, 2 m length) were dipped in the mucin solution, withdrawn and image clarity was determined by visualizing a checkerboard pattern after every dip. The image analysis performed was the same as for the blood dip experiments and is described in detail in Chapter 3 below.

Contamination with cellular debris

Cellular debris is often collected in endoscopic procedures and during bronchoalveolar lavages in particular. In order to mimic this effect and understand whether cellular debris induces lens occlusion, we suspended 60 million CT26 colon cancer cells in a 1.5 mL solution of Roswell Park Memorial Institute (RPMI) 1640 medium supplemented with 10% Fetal Bovine Serum and 1% penicillin streptomycin and dipped the endoscope into this solution. The image clarity was determined by visualizing a checkerboard pattern every ten dips. The image analysis is described in detail in Chapter 3 below.

Cell toxicity experiments

Effect of silica nanoparticles. Following the International Organization for Standardization's (ISO) guidelines for *in vitro* toxicity tests (1), OVA D1 mesenchymal stem cells were cultured in Dubecco's Modified Eagle Medium (DMEM) supplemented with 10% Fetal Bovine Serum (FBS), antibiotic/antimycotic solution, sodium pyruvate, and bovine insulin following American Type Culture Collection established protocols. Apart from being commonly used in toxicity studies (2), mesenchymal stem cells were chosen as the cell line in an effort to generalize the toxicity to various tissues encountered in endoscopy. A confluent flask of cells was trypsinized and seeded in a 24-well plate at 100 000 cells/well. Cells were allowed to adhere for 24 h in a cell culture incubator at 37°C, 5% CO_2 and 95% relative humidity. They were subsequently washed with Hank's Balanced Salt Solution (HBSS) buffer, and incubated with varying concentrations of silica nanoparticles (0 wt.%, 0.003 wt.%, 0.025 wt.%, 0.05 wt.%, and 1 wt.%) suspended in DMEM. Each concentration was tested in triplicate. The cells were incubated at 37°C for another 24 h. After this incubation period, the culture medium was removed from the wells and the cells were washed with HBSS. 1 mL of DMEM solution (without serum) containing 0.5 μM Calcein AM and Ethidium homodimer-1 was added to each well. The cells were incubated in this solution for 20 min before imaging was performed with a Carl Zeiss Axiovert 40 CFL fluorescent microscope.

Effect of silicone oil/fluorinated oil. 10 μL/cm^2 silicone oil was added to the layer-by-layer assembled silica nanoparticle-coated glass surface that was cut in 0.5 cm x 0.5 cm square pieces and spin-coated at 5000 rpm for 1 min to remove excess lubricant. A droplet of water was added to the surface to check for slipperiness after spin coating. After confirmation that the samples were still slippery, the unlubricated glass samples and the lubricated samples were UV-treated for 5 min and placed in a 24-well plate. Trypsinized mesenchymal stem cells were added to each well at 100 000 cells/well. Cells were allowed to adhere for 24 h in a cell culture incubator at 37°C, 5% CO_2 and 95% relative humidity. The live/dead stain was performed after 72 h using Calcein AM, and Ethidium homodimer-1 was added at a 0.5 μM concentration in each well. The culture media was not removed prior to adding the live/dead stain in order to perform the staining in such a way that no cells would be removed from the wells. This particular method was used to obtain the results depicted in Fig. 3.

The toxicity data were collected slightly differently for Fig. S10. Cells were seeded onto a transwell insert, which was placed into contact with the samples. The cells were stained after

24 h using the live/dead stain. The brightfield images shown are of cells that were directly in contact with the coated substrate. This type of direct contact study was performed in an effort to satisfy the medical material *in vitro* toxicity tests outlined by the ISO standard guidelines.

Bacterial attachment assays

To make bacterial stock solution, 4-6 colonies of *E. coli* were scraped from a streaked agar plate and vigorously swirled in 2 mL of Minimal media (M63 media from VWR Amresco Life Science). This solution was incubated overnight in a shaker at 37°C. The samples were then inoculated using a 1:100 volume ratio of stock bacteria solution to Minimal media. The inoculated samples were incubated for 24 h at 37°C. 1 cm x 1 cm glass slides (2 mm thickness) coated with silica particles, functionalized with n-decyltrichlorosilane and infused with 10 cSt silicone oil were incubated with *E. coli* cultured in Minimal media for 24 h. Plain glass was also incubated for 24 h and served as a control. The samples were removed from solution and stained with crystal violet (CV). Sonicating the CV stained samples in ethanol and measuring the absorbance of the solution at 590 nm further quantified the CV staining.

Mechanical tests

A coated Eggsnow scope (5.5 mm diameter, 2 m length) was infused with 3 μL of 10 cSt silicone oil. The excess oil was removed by holding the coated edge to a Kim wipe for excess oil absorption. A 20 μL volume polypropylene pipette tip was used to form multiple scratches spanning the entire diameter of the coated surface. Dipping tests in whole porcine blood were subsequently performed. The image clarity was determined by visualizing a checkerboard pattern every ten dips. The image analysis is described in detail in Section 3 below.

***Ex vivo* lung airway inspection**

The explanted porcine lung for the studies presented in Fig. 4*A* was obtained from a butcher store (Research 87 in Boylston, MA). Coated and uncoated Eggsnow Endoscopes were used to visualize the inside of the lungs.

***In vivo* airway inspection and biopsy procedures**

A Yorkshire female pig (weight 40-50 kg) was given general anesthesia and intubation with an 8.0-9.0 ET tube. It was mechanically ventilated with a bronchoscope adaptor to allow bronchoscopy. During this time, the animal was maintained in anesthesia with Fentanyl and propofol adjusted based on clinical signs (Fentanyl IV 50-100 μg/kg/hour for 2 h, Propofol IV 0.3-0.5 mg/kg/min for 2 h).

The bronchoscope was introduced to perform airway inspections and biopsies. The Olympus Bronchoscope (EXERA BF-160) used in the *in vivo* bronchoscopy experiments is part of the clinical setup at Beth Israel Deaconess Medical Center. The procedures were performed by three operators.

The endobronchial biopsy was performed with standard biopsy forceps under direct visualization. A 1.8 mm forceps biopsy device was fed through the working channel (OD of 2 mm) on the bronchoscope (OD of 6.7 mm). The operator selected an area and the biopsy was done superficially with 1 single bite of the tissue (3 samples were collected). Three biopsies were performed by each operator using the coated bronchoscope in the left lung of a ventilated pig *in vivo*. The same three procedures were performed by each operator using an uncoated bronchoscope in the right lung.

During the transbronchial biopsy, the bronchoscope was advanced into the area of the lung to be biopsied. The forceps were advanced via the working channel and pushed out as far as possible. Then the forceps were retracted 1 cm to avoid a biopsy of the pleura. The forceps were opened, advanced and closed. They were then removed and the sample retrieved. This sequence was repeated 3 times. During the transbronchial brushing, the brush was advanced via the working channel while retracted in its protective sheath. Once the bronchoscope was advanced as far as possible into the area of the lung to be brushed, the brush in the protected sheath was pushed out of the working channel. Ten agitations were performed in the area of interest. Then the brush was retracted into its sheath (closed) and removed from the working channel and the procedure was repeated two more times.

The whole apparatus (bronchoscope and biopsy device) was retracted enblock via the ET tube. The coated bronchoscope was used first with 6 µL of silicone oil. All procedures involving the coated bronchoscope were performed in the left lung. The coverslip was then removed, the bronchoscope was wiped with a Clorox wipe, washed in ethanol, dried and re-inserted into the right lung where the same biopsy procedure was repeated with an uncoated bronchoscope. A blind study could not be performed because of a limitation to the number of bronchoscopes available for use. Therefore, only one bronchoscope could be used to test the performance of both the liquid-infused coating and the unmodified control. Three coated bronchoscopes were used and operated by three physicians.

2. Modification of the endoscopes used

A 5.5 mm diameter pipe inspection camera was initially used to characterize the physico-chemical properties of the surface coating in the *in vitro* blood and mucus dips, as well as in the *ex vivo* lung experiment. These scopes were 5 mm in diameter and chosen to be similar in size to the bronchoscopes used in the *in vivo* experiments. A glass coverslip was coated and attached on the surface of the camera using PDMS (Fig. S1*A, B*). The subsequent *in vivo* experiments were performed using a 6.7 mm diameter bronchoscope that was modified with a 6 mm glass coverslip cut in the shape of a crescent to fit over the camera lens and light sources while leaving the working channel exposed (Fig. S1*C*). The coverslip was coated with the liquid-infused coating and attached onto the bronchoscope using PDMS. Three modified bronchoscopes were used and operated by three physicians. All the procedures were repeated multiple times.

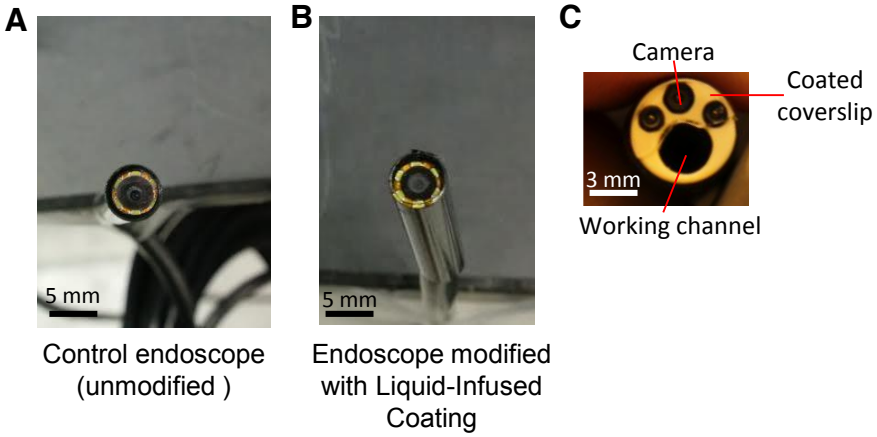

Fig. S1. Schematic of endoscope coating process. The unmodified (*A*) and the modified (*B*) pipe inspection camera used in the *in vitro* blood and mucus dipping experiments and the *ex vivo* experiment with lung surfactant. (*C*) A bronchoscope is modified with a disposable, coated glass coverslip.

3. Image analysis of the field of view for dipping experiments

ImageJ was used to subtract the background of the image at a threshold of 10 pixels. The following options were checked:

- light background
- separate colors
- sliding paraboloid
- disable smoothing

The image was converted from Fig. S2*A* to S2*B*.

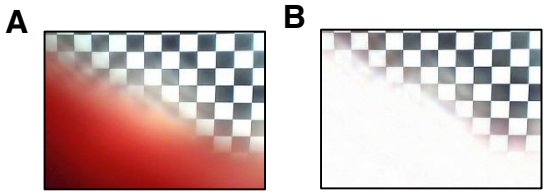

Fig. S2: The original image (*A*) is changed to subtract the background (*B*).

Matlab was used to count the number of excess white pixels, which corresponds to the area obscured assuming that an unobstructed image has 50% black pixels and 50% white pixels. The following script outputs values for the excess white region.

```
clear all
clc
Folder='/Users/steffisunny/Documents/Aizenberg Group/Endoscope Project/All Blood Dip Experiments/500cSt silicone oil_06-10-15';
i=0;
for imagenum=0:10:100
i=i+1;
   Picture = [Folder,'/',num2str(imagenum),'_6_imageJ10.jpg'];
original=imread(Picture);
greyimg=[]
greyimg = im2bw(original, graythresh(original));
numberOfPixels(i) = numel(greyimg);
numberOfBlackPixels(i) = sum(sum(greyimg == 0));
numberOfWhitePixels(i) = sum(sum(greyimg));
percentwhite(i)=numberOfWhitePixels(i)/numberOfPixels(i)*100
percentblack(i)=numberOfBlackPixels(i)/numberOfPixels(i)*100
approximateblurredregion(i)=percentwhite(i)-percentblack(i)
end
```

4. Re-lubrication experiments

As shown in the main text, the 10 cSt silicone oil maintains a clear visual field up to 100 dips in whole porcine blood. Fig. S3 below demonstrates that following these 100 dips, the pipe inspection endoscope can be gently rinsed, re-lubricated and dipped in whole porcine blood another 100 times. Fig. S3 demonstrates the clarity of dips 0, 20, 40, 60, 80, and 100 after re-lubrication.

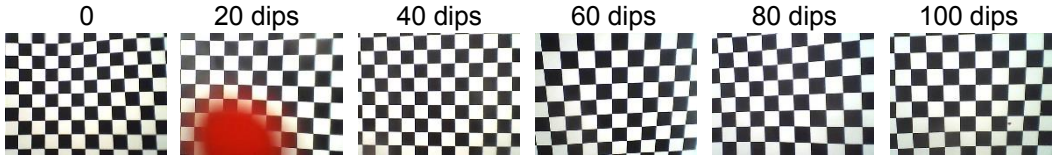

Fig. S3. Re-lubrication of surface coating after 100 dips in porcine blood with 10 cSt silicone oil.

5. Blood-repellency of coatings infused with different lubricants

As mentioned in the main text, the coating can fail if the contaminating liquid (blood in our case) comes into contact with the underlying silica network and becomes pinned due to mismatch in surface chemistry. The conditions for a stable, intercalated lubricant film between the liquid and underlying solid substrate have been described elsewhere (5).

The in vitro tests revealed that of all the viscosities and oil chemistries that were tested, 10 cSt silicone oil consistently gave better results than the Vitreon or PFPE variants. We would like to emphasize that silicone oil is not objectively better than the Vitreon or PFPE variants at repelling biological fluids (blood in this particular case) but the specific combination of the n-decyltrichlorosilane surface chemistry and silicone oil results in the most effective coating whereas 13F-functionalized silica and Vitreon/PFPE oil combination results in faster failure upon multiple exposures to blood.

This was further corroborated by performing contact angle and force measurements of a blood droplet on the n-decyltrichlorosilane-functionalized surface infused with silicone oil and the 13F-functionalized surface infused with Vitreon (Fig. S4). For a coating hydrophobized by vapor phase deposition of n-decyltrichlorosilane or 13F and infused with silicone oil and fluorinated oils, respectively, the blood droplet forms a higher contact angle with the underlying solid substrate for the silicone oil-infused n-decyltrichlorosilane-functionalized surface compared to Vitreon-infused 13F-functionalized surface. Higher contact angle indicates greater repellency. This is true for a flat piece of functionalized, oil-coated glass substrate ($\theta = 160^o$ for silicone oil, 120^o for Vitreon, top row, Fig. S4A), as well as for functionalized oil-coated textured silica nanoparticles surface described in this study ($\theta = 180^o$ for silicone oil, 170^o for Vitreon, bottom row, Fig. S4A). The blood droplets (in all cases 10 µl in volume) were illuminated with a bright LED light from the side; the presence of a micrometer-thick film beneath the droplet for the silicone oil-infused nanoparticulate coating developed in this study allows light to pass through and this is captured by a high-resolution camera (indicated by a white asterisk and a red arrow in Fig. S4A). The droplet is cushioned on a micrometer-thick layer of silicone oil. In contrast for a Vitreon-infused coating, the blood droplet is in contact with the silica network, preventing any light from passing through.

This explains why a blood droplet is much more mobile on a silicone-infused coating than on a Vitreon-infused coating. The mobility of the droplet can be quantified by using a cantilever-based force sensor (Fig. S4*B*). Briefly, a 2 µl blood droplet was held by a capillary tube (PMMA, length L = 10 mm, inner and outer radii, $r_{i,o}$ = 0.29, 0.36 mm) while moving the surface with a motor at speed, U = 0.4 mm/s. The force acting on the droplet, F, is proportional to the deflection, Δz, i.e. F = k Δz, where k = 6.3 µN/mm. A similar experimental set-up has been described in detail elsewhere (6). For silicone-infused coating, the maximum force experienced by the blood droplet is < 10 µN, less than the droplet weight, W = 20 µN. For Vitreon-infused coating, the pinning force is > 40 µN, more than twice of W and more than the maximum force measurable with the system. This also explains why silicone oil-infused coating (viscosity = 10 cSt) can maintain its blood-repellency with close to 100% visibility for at least 100 dips in whole porcine blood, while the Vitreon-infused coating (viscosity = 8 cSt) maintains 100% visibility for only four dips at which point ~50% of the visual field is occluded by blood (Fig. S5*A*).

Higher viscosity perfluorocarbons were tested and determined to increase the longevity of the coating. The commercially available perfluoropolyether, Krytox 105 (550 cSt) outperforms Vitreon (8 cSt) and Krytox 103 (80 cSt) by ~30 dips and ~20 dips, respectively. This is because the time required for the blood to squeeze out the lubricant layer and therefore come into contact with the solid substrate is inversely proportional to lubricant viscosity.

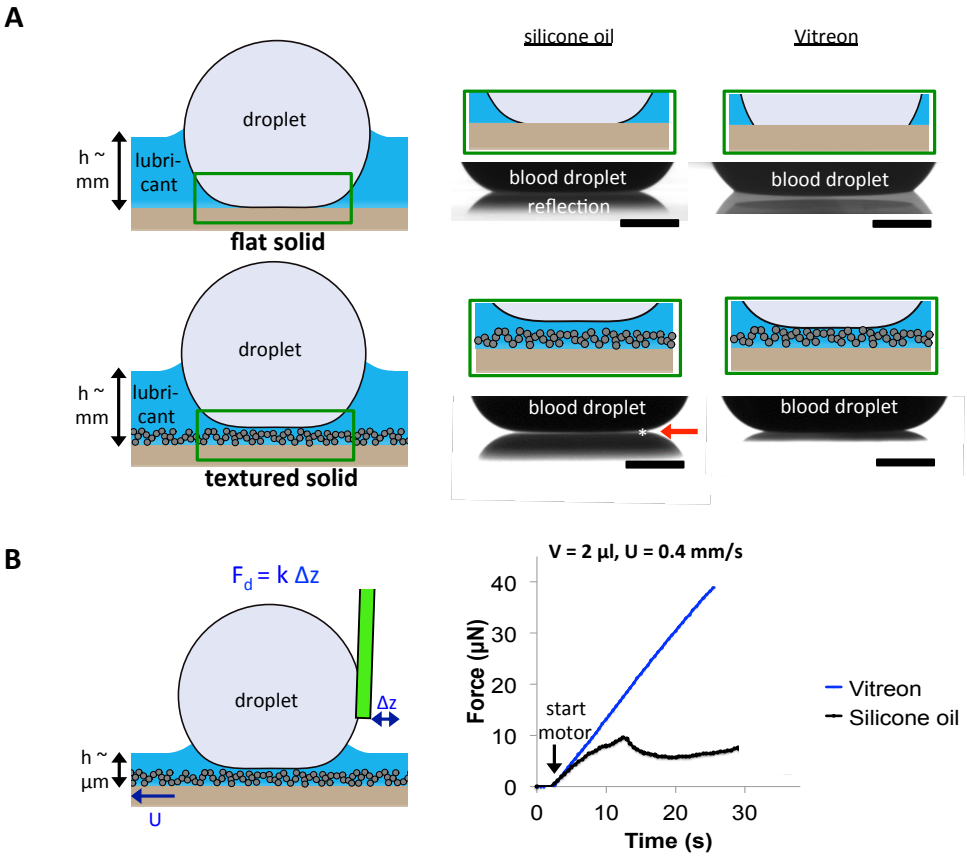

Fig. S4. Evaluating coating stability when using silicone oil lubricant compared to Vitreon. (*A*) This schematic representation of our experimental setup shows a static droplet of blood on the coating with a millimeter-scale lubricant over-layer while illuminated sideways using LED light. Light passes through the micrometer-thick lubricant film sandwiched between the droplet and silica network for silicone-oil

infused coating (bottom row left, marked by * and indicated by a red arrow), but is completely blocked out for Vitreon-infused coating as the droplet is in contact with the silica network (bottom row right). (*B*) A capillary tube is used to measure the force required to un-pin a 2 μL droplet of blood from a silicone oil-infused and Vitreon-infused surface.

After > 100 dips, the silicone oil-infused coating starts to lose its blood repellency, as the lubricant is depleted due to shear force. Reapplying the lubricant will, however, restore its performance (See Fig. S3 and main text). In contrast, for fluorinated oil-infused surface, after a pinning point forms on the fluorinated coating, complete loss in visibility occurs almost immediately with permanent degradation of performance (Fig. S5). A wash with de-ionized water and re-lubrication only leads to continued clarity for two more dips before failure occurs again, indicating a compromised surface functionality, presumably from adsorption of proteins (Fig. S5*C*).

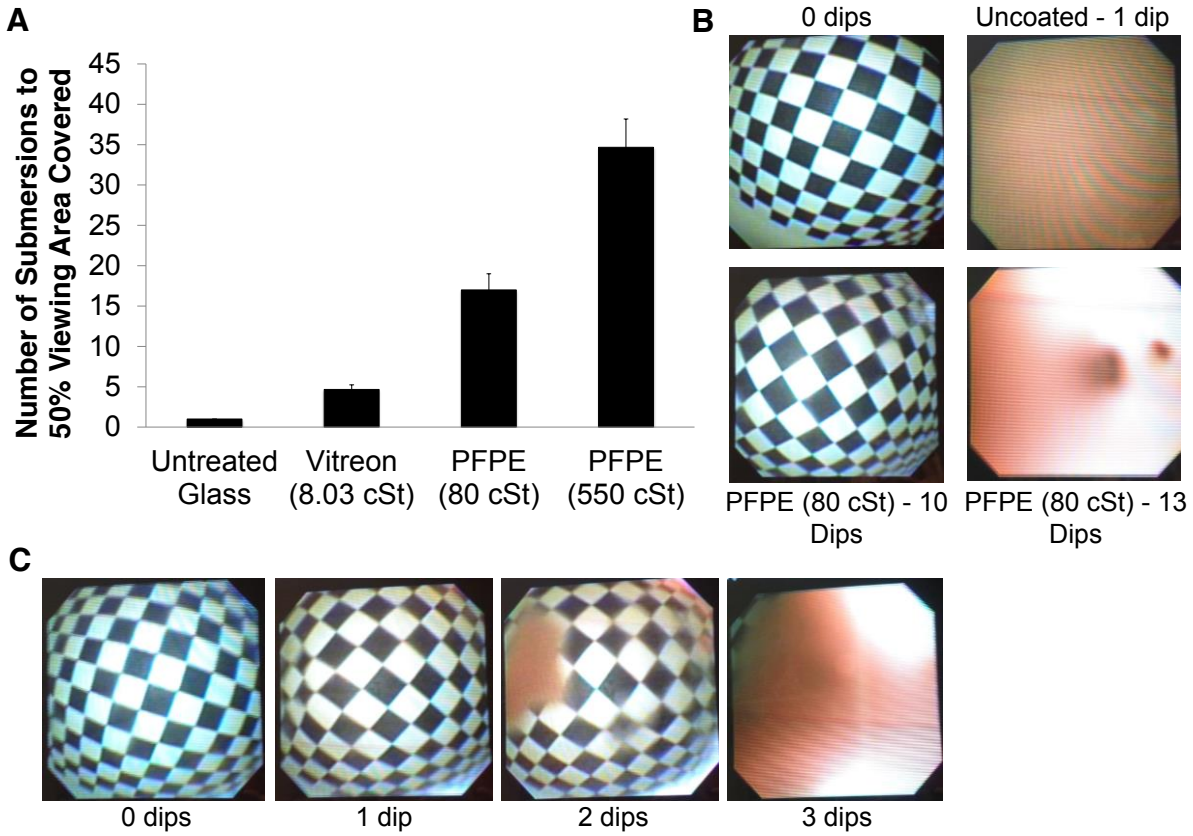

Fig. S5. Whole porcine blood dipping experiments with varying viscosity of fluorinated lubricants. All experiments were performed with a sample repeat of three. (*A*) Dipping was performed in whole porcine blood using scopes coated with Vitreon (8 cSt), PFPE (80 cSt) and PFPE (550 cSt). (*B*) The uncoated scope fails immediately after one dip while PFPE (80cSt) oil allows for repellency for more than 10 dips before failure. (*C*) Re-lubricating the endoscope prolongs the performance for 2-3 dips in blood before complete failure.

6. Mucus dipping experiments with PFPE-coated endoscopes

We performed additional mucus dipping experiments with Vitreon, 80 cSt PFPE oil, and 550 cSt PFPE oil (Fig. S6). As expected, we found from this experiment that failure occurred much sooner for the Vitreon/PFPE variants compared to the silicone oil. The Vitreon coating (8 cSt) failed on average after 8 dips in mucus solution compared to 20 dips for the 10 cSt silicone oil coating. The highest viscosity PFPE oil failed after an average of 16 dips compared to 21 dips for the 350 cSt silicone oil. Failure was defined as the number of dips where three subsequent dips did not restore the visual field (and therefore, the lack of clearance could not be attributed to slow viscous dissipation). Subsequent addition of a droplet of water on the surface resulted in pinning, also indicating failure. The data points on the plots for each of the replicates end when complete failure of the coating occurred and visibility could not be restored.

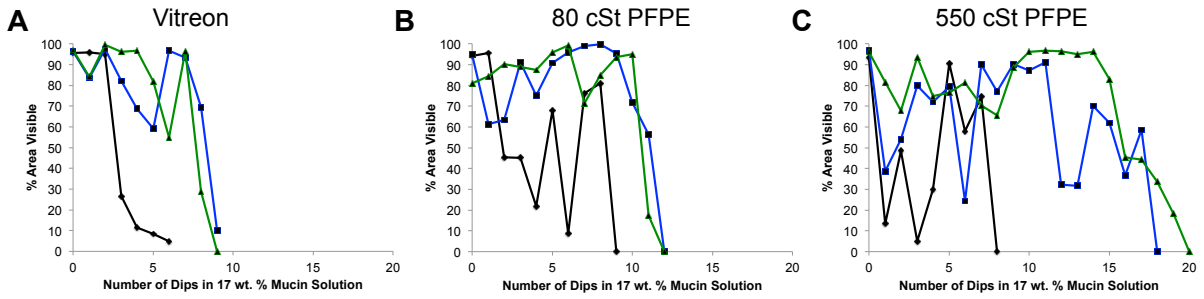

Fig. S6. Characterization of the visual field during mucus dipping experiments with PFPE-coated and untreated endoscopes. *(A)* Vitreon, *(B)* 80 cSt PFPE, and *(C)* 550 cSt PFPE. 17 wt.% mucus solution was used. All experiments were performed in triplicates. Replicates = 1 (blue), 2 (green), 3 (black) correspond to each sample tested.

7. Performance of un-functionalized silica nanoparticle layers

As discussed in the previous section, the surface chemistry has to be matched for optimal blood-repellency of the coating. When silicone oil is infused into the un-functionalized silica nanoparticle coating, its native surface functionality appears to be sufficient for the oil to remain entrapped only for 20 dips in blood before the repellency properties fail (using n-decyl-silane surface functionality, the same coating survives for upwards of 100 dips). The same silica particle coating without surface functionalization infused with perfluorocarbon oil fails almost instantly indicating that there is no matching surface chemistry between the oil and the coating to ensure coating longevity (Fig. S7).

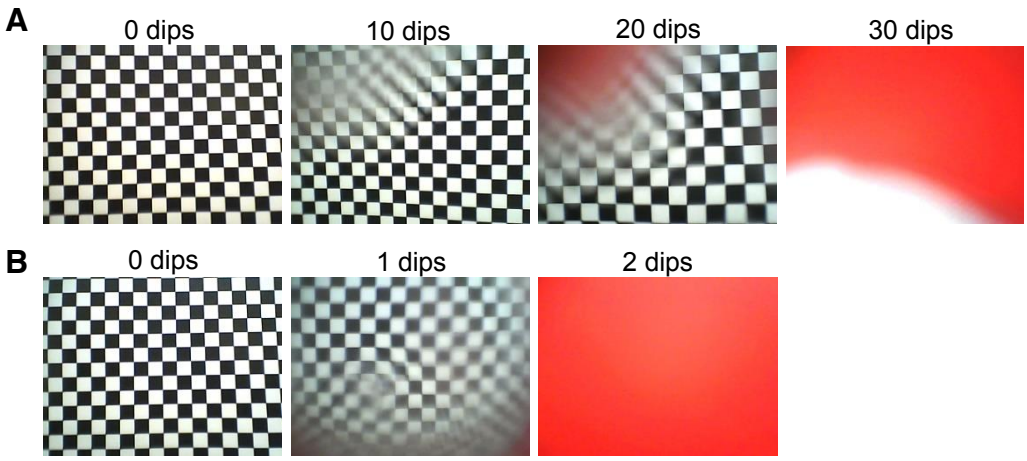

Fig. S7. Silicone oil and perfluorocarbon oil on un-functionalized silica layers. Dipping was performed in whole porcine blood using scopes coated with 20 layers of silica particles and (*A*) 10 cSt silicone oil and (*B*) PFPE 80 cSt. The silica particles were not functionalized.

8. Difference in longevity of the coatings infused with 10 cSt and 350 cSt silicone oil

Typically in flexible bronchoscopy, the endoscope may be simultaneously used for both therapeutic purposes (such as clearing a mucus plug) and diagnostic purposes (such as biopsies from lymph nodes), which typically leads to blood release within the lungs (7, 8). This combined interaction with both mucus and blood can deteriorate the longevity of the coating. In order to mimic this scenario, we re-lubricated the endoscopes after the dipping experiments in mucus and performed another series of blood exposure. As shown in Fig. S8*A*, the 10 cSt oil fails at 13 dips while the 350 cSt oil sustains clarity for 50 dips. This indicates that despite 10 cSt silicone oil typically outperforming the higher viscosity oils, there may be occasions when choosing a higher viscosity lubricant is beneficial depending on the procedure and the predicted severity of the fouling.

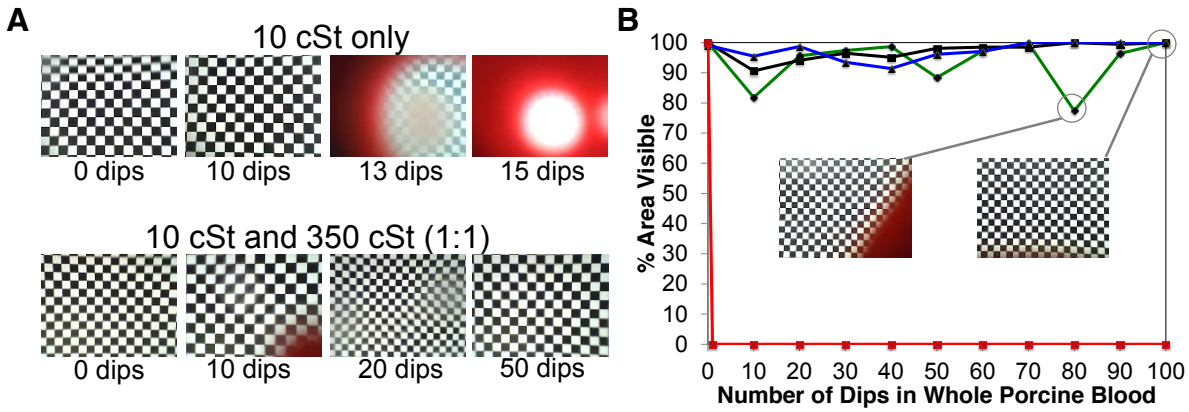

Fig. S8. (*A*) Performance of silicone oil coatings in blood dipping experiments after submersions in 17 wt.-% mucin solution. The 10 cSt silicone oil coating fails after 13 dips while the 1:1 ratio provides a clear image even after 50 dips. (*B*) Evaluating the repellency properties of a 1:1 ratio of 10 cSt and 350

cSt silicone oil coating in whole porcine blood with three replicates. A combined repellency effect of whole blood is achieved: the droplets are highly mobile on the surface as seen in the 10 cSt data and longevity is improved due to the 350 cSt oil.

9. Approximation of the amount of silica particles in the coating and image analysis in toxicity experiments

As shown in (4) using Quartz Crystal Microbalance data, 10 layers of silica particles consist of roughly less than 1.2×10^4 ng/cm^2 (4). We estimate that on a 6 mm diameter coverslip containing 20 layers of particles, there will be roughly 6.8×10^{-6} g of particles. This corresponds to 0.00068 wt.%. However, it should be kept in mind that a bronchoscope has a 2 mm working channel that is not coated. Therefore, this value is an over-estimation.

A macro file was created in ImageJ containing the following commands:

```
run("8-bit");
run("Enhance Local Contrast (CLAHE)", "blocksize=25 histogram=2048 maximum=20
mask=*None* fast_(less_accurate)");
run("Auto Threshold", "method=MinError1 white"); run("Select All");
run("Measure");
```

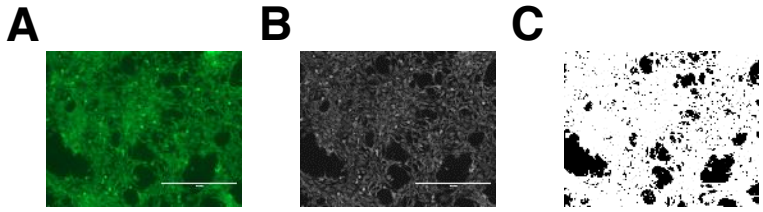

Fig. S9. The original image (*A*) is changed to a grey scale with enhanced local contrast (*B*). Using auto threshold, the cell coverage is output in white (*C*).

The command Measure returns the % Area value of the white regions. The same process is performed for the dead stain in red. However, the auto threshold method used for this stain is Triangle.

10. Toxicity of PFPE (80 cST)

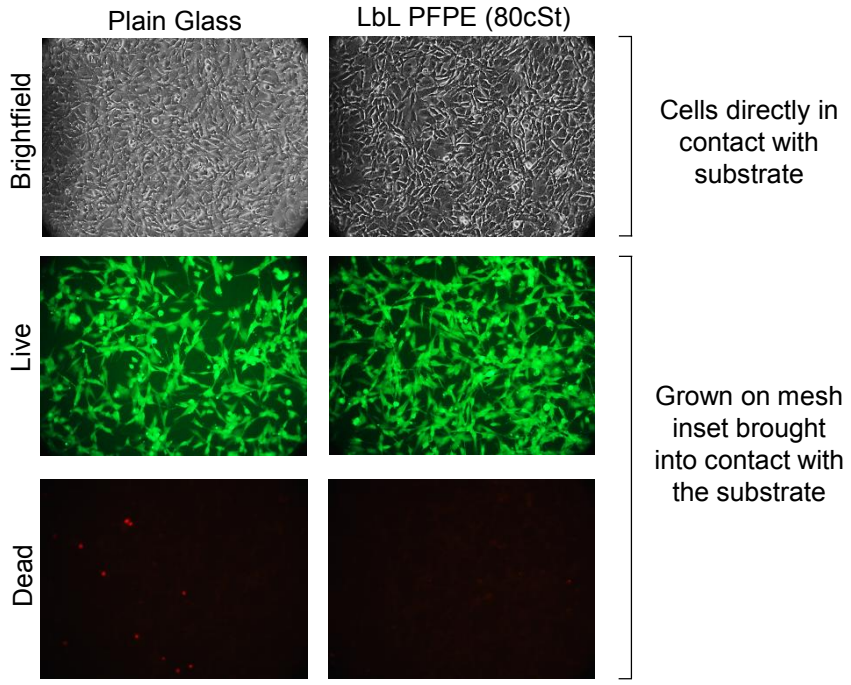

Fig. S10. Toxicity study of PFPE (80cSt) infused layer-by-layer (LbL) assembled silica particle surfaces. Brightfield images show mesenchymal stem cells that were in contact with plain glass and PFPE-infused LbL surfaces for 24 h of incubation. Calcein AM was used to stain live mesenchymal stem cells grown on a polymer mesh in contact with plain glass and PFPE-infused LbL glass in a transwell plate. Cells thrive in the presence of both the plain glass control and the liquid-infused coating. There are negligible dead cells.

11. Preventing bacterial adhesion

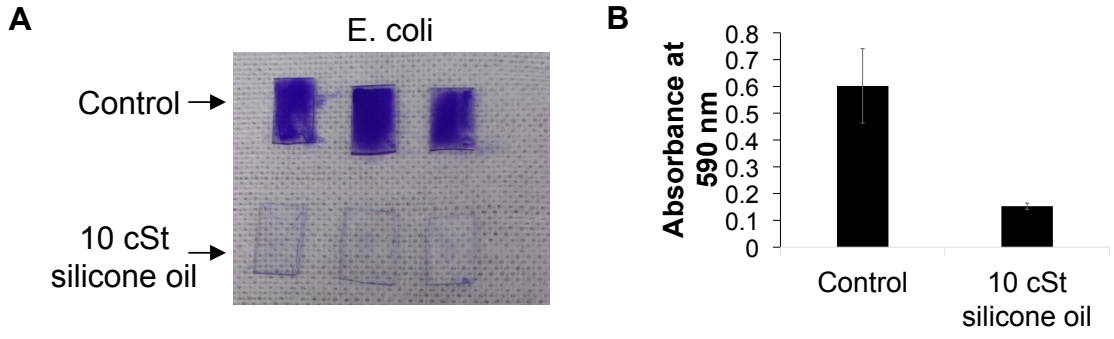

Fig. S11. Bacterial adhesion on a coated and plain glass slide. *(A)* Crystal violet staining of plain glass (Control) and 10 cSt silicone oil-infused silica nanoparticles coating after 24 h incubation with *E. coli*. *(B)* The quantification of crystal violet staining. Samples coated with silica nanoparticles, functionalized and infused with silicone oil significantly outperform uncoated controls in their ability to reduce bacterial attachment.

12. Lens occlusion by cellular debris

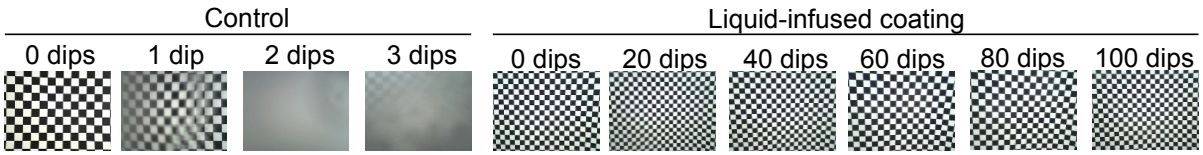

Fig. S12. Dipping of uncoated endoscope and coated endoscope in a cell suspension. As expected, the vision is obstructed in the uncoated control case after 2 dips but the coated endoscope maintains clarity for at least 100 dips.

13. Stability in a low pH environment

We repeated the blood dip experiments for the 10 cSt silicone oil coating after incubating the endoscope in a pH 2 aqueous solution for 10 min (pH adjusted using HCl). After incubation, the endoscope was immediately submerged multiple times in whole porcine blood. The visual field remained completely clear for 100 dips indicating that low pH (such as what is found in the stomach) does not destabilize the coating (Fig. S13). Fluorinated coatings have also been tested in low pH conditions and shown to not degrade (9).

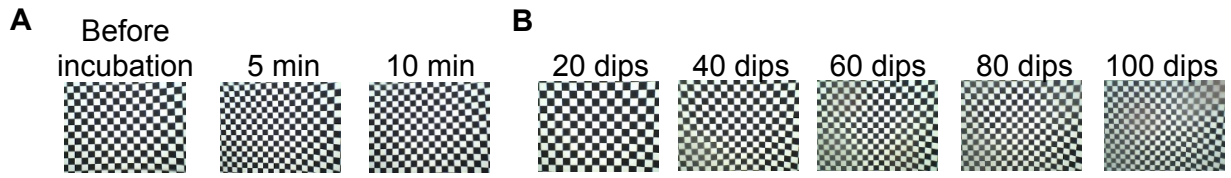

Fig. S13. Stability of the coating in a low pH environment. *(A)* Incubation of 10 cSt silicone oil infused endoscope in pH 2 solution (mimicking the acidity of the stomach) for 5 min and 10 min. *(B)* After the 10 min incubation, the 10 cSt silicone oil infused coating was subsequently dipped in whole porcine blood to check if the performance of the coating had been disturbed.

14. Mechanical damage tolerance

The coating repels blood after vigorous scratching with a pipette tip. This level of scratching mimics the potential scratches endured by an endoscope lens during endoscopy such as when the endoscope passes through the plastic flaps of a patient's intubation tube.

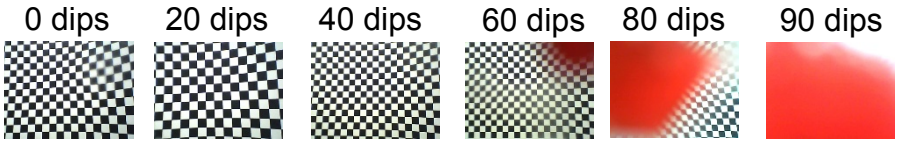

Fig. S14. Visual clarity of 10 cSt silicone oil coated endoscope dipped in porcine blood after vigorous scratching using a plastic pipette tip.

15. Broader implications

Fig. S15*A-C* show dipping of a coated and regular endoscope in crude oil, algae solution, and sewage mimetic solution. The results show minimal visual disruption for the liquid-infused coating for more than 100 dipping events and nearly immediate failure of the uncoated endoscopes in these conditions. Although we envision multiple potential applications for our transparent antifouling coatings in camera-guided instruments and optical components, we hope these brief demonstrations illustrate the possible broader implications of this coating. More in-depth studies of these coatings to prevent marine fouling and sewage contamination are currently underway in our group.

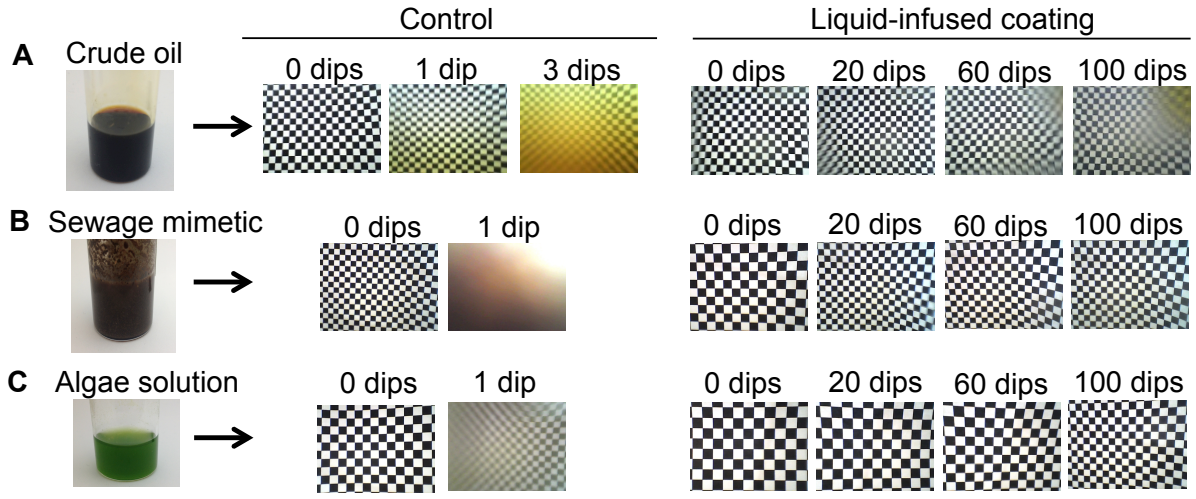

Fig. S15. Preventing visual field occlusion by *(A)* crude oil, *(B)* sewage mimetic, and *(C)* algae solution using 10 cSt silicone oil-infused coating.

Supporting Information References:

1. 10993-5 IS (2009) *Biological Evaluation of Medical Devices: Part 5 Tests for In Vitro Cytotoxicity*).
2. Davila JC*, et al.* (2004) Use and Application of Stem Cells in Toxicology. *Toxicology Science* 79(2):214-223.
3. Rogers CS*, et al.* (2008) The porcine lung as a potential model for cystic fibrosis. *American Journal of Physiology - Lung Cellular and Molecular Physiology* 295(2):L240-L263.
4. Sunny S, Vogel N, Howell C, Vu TL, & Aizenberg J (2014) Lubricant-Infused Nanoparticulate Coatings Assembled by Layer-by-Layer Deposition. *Advanced Functional Materials* 24(42):6658-6667.
5. Smith JD*, et al.* (2013) Droplet mobility on lubricant-impregnated surfaces. *Soft Matter* 9(6):1772-1780.

6. Pilat, D. W., *et al.* (2012) Dynamic measurement of the force required to move a liquid drop on a solid surface. *Langmuir*, *28*(49), 16812-16820.
7. Rand IAD*, et al.* (2011) British Thoracic Society Guidline for Advanced Diagnostic and Therapeutic Flexible Bronchoscopy in Adults. *Thorax* 66:iii1-iii21.
8. Rand IAD*, et al.* (2013) British Thoracic Society Guideline for Diagnostic Flexible Bronchoscopy in Adults. *Thorax* 68:i1-i44.
9. Epstein AK., *et al*. (2012) Liquid-infused structured surfaces with exceptional anti-biofouling performance. *Proceedings of the National Academy of Sciences of the United States of America* 109(33):13182-13187.